Supporting Information

Colorimetric Recognition of Lanthanide Ions with a Complexometric Indicator Array

Tiantian Zhang, Xiuzhi Zhuo, Guoyue Shi, Min Zhang*

Contents

Section 1: Experimental Section

Materials and Reagents

Eriochrome Black T (EBT), Alizarin Red (AR), hydrochloric acid (HCl), Tris (hydroxymethyl) methyl aminomethane ($H_2NC(CH_2OH)_3$), $La(NO_3)_3·6H_2O$, $Ce(NO_3)_3·6H_2O$, $Pr(NO_3)_3·6H_2O$, $Nd(NO_3)_3·6H_2O$, $Sm(NO_3)_3·6H_2O$, $Eu(NO_3)_3·5H_2O$, $Gd(NO_3)_3·6H_2O$, $Tb(NO_3)_3·5H_2O$, $Dy(NO_3)_3·6H_2O$, $Ho(NO_3)_3·5H_2O$, $Er(NO_3)_3·5H_2O$, $Tm(NO_3)_3· 5H_2O$, $Yb(NO_3)_3·5H_2O$, $Lu(NO_3)_3·6H_2O$ were purchased from Diyang Chemical Co. Ltd. (Shanghai, China). Tris-HCl buffers at pH 7.4 and 8.5 (100mM) were prepared using metal-free reagents in distilled water purified by a Milli-Q water purification system. All chemicals used in this work were analytical purity grade and obtained from commercial sources and directly used without further purification.

Equipment and software

The pH values are measured by a pH-meter (SevenEasy, METTLER TOLEDO, Switzerland). Absorption spectra were recorded by a microplate reader (infinite M200 pro, TECAN, Switzerland) using a transparent 384-well microplate (Corning, U.S.A.). The data processing and drawing of PCA diagram were completed by Statistical Product and Service Solutions 23.0 software (IBM) and GraphPad Prism 8.0 (San Diego, CA).

Measurement of maximum absorption peak

The maximum absorption peak position of EBT solution (final concentration: 50 μM) was measured in buffer solutions at pH 7.0 and 8.4. Then, lanthanide ions (final concentration: 50 μM) were added to measure the UV-Vis absorption spectrum.

AR solution (final concentration: 50 μM) was treated in the same way. The maximum absorption peak position and the UV-Vis absorption spectrum were measured with or without lanthanide ions added.

Preparation of sensor array

EBT solutions (500 μM) were mixed respectively with buffer solutions at pH 7.4 and 8.5. AR solutions (500 μM) were treated in the same way. They were placed on the oscillator for 1 min at room temperature, fabricating four different sensors ($EBT_{7.4}$、$EBT_{8.5}$、$AR_{7.4}$、$AR_{8.5}$).

14 kinds of lanthanide ions were added to four different sensors ($EBT_{7.4}$、$EBT_{8.5}$、$AR_{7.4}$、$AR_{8.5}$) , and mixed evenly to construct sensor array. The final concentrations of sensors, rare earth ions and buffers were both 50 μM. All samples were placed at room temperature for 15 min to obtain the original sample number matrix (4 receptors × 14 lanthanide ions × 5 replicates).

The UV-Vis absorption spectra were measured by microplate reader. The absorption wavelength was 530 nm.

Study of sensitivity

The solution of Ce^{3+}, Dy^{3+}, Tm^{3+}(500 μM) was diluted to samples at different concentrations. The diluted solution was added to four different sensors ($EBT_{7.4}$、$EBT_{8.5}$、$AR_{7.4}$、$AR_{8.5}$) respectively, and mixed well to determine the UV-Vis absorption diagram.

Study of selectivity

Transition metal ions (Fe^{3+}, Co^{2+}, Ni^{2+}, Cu^{2+}, Zn^{2+}, Hg^{2+}), alkaline-earth metal ions (Mg^{2+} and Ca^{2+})， anions (S^{2-}, $S_2O_8^{2-}$, SO_4^{2-}, NO^{2-}, $EDTA^{2-}$), and amino acids (Gly, Lys, Arg, His) were chosen as interferents to test the selectivity.

Discrimination of lanthanide ions mixture with different proportions

The mixture of La^{3+} and Ce^{3+} with different molar ratios (La^{3+}/Ce^{3+} = 50/0, 40/10, 30/20, 20/30, 10/40, 0/50, 50 μM in total) was added to $EBT_{7.4}$、$EBT_{8.5}$、$AR_{7.4}$、$AR_{8.5}$ respectively to obtain UV-Vis absorption diagram. The mixture of Ce3+ and Gd3+ with different molar ratios (Ce^{3+}/Gd^{3+} = 50/0, 40/10, 30/20, 20/30, 10/40, 0/50, 50 μM in total) was operated in the same way stated above.

Identification of lanthanide ions in real samples

To explore the application of the sensor array in actual sample analysis, we used river water and tap water as samples for determination. The river water sample used in this experiment was collected from Cherry River, a river in Shanghai, China (31.2°N, 121.5°E). The river water was filtered by a 0.22 μm membrane syringe filter.

Section 2: UV-Vis absorption spectra of EBT/AR-Ln^{3+}

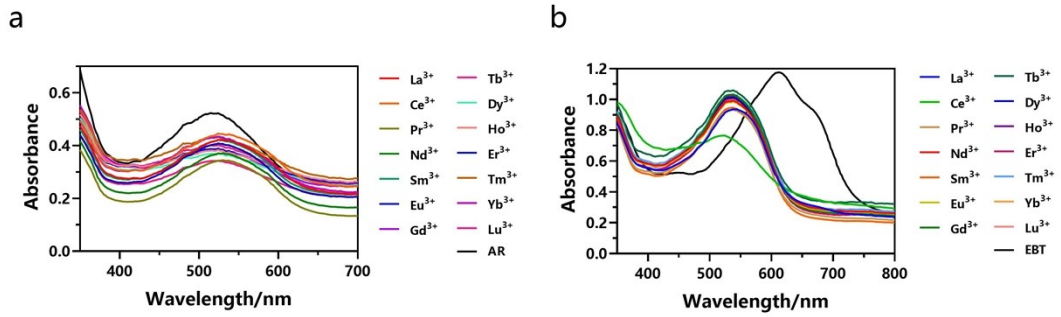

Figure S1. Absorption spectra of EBT/AR (50 μM) along with spectral changes after addition of various Ln^{3+} ions (50 μM each) in water at room temperature at (a) AR pH 7.4; (b) EBT pH 7.4.

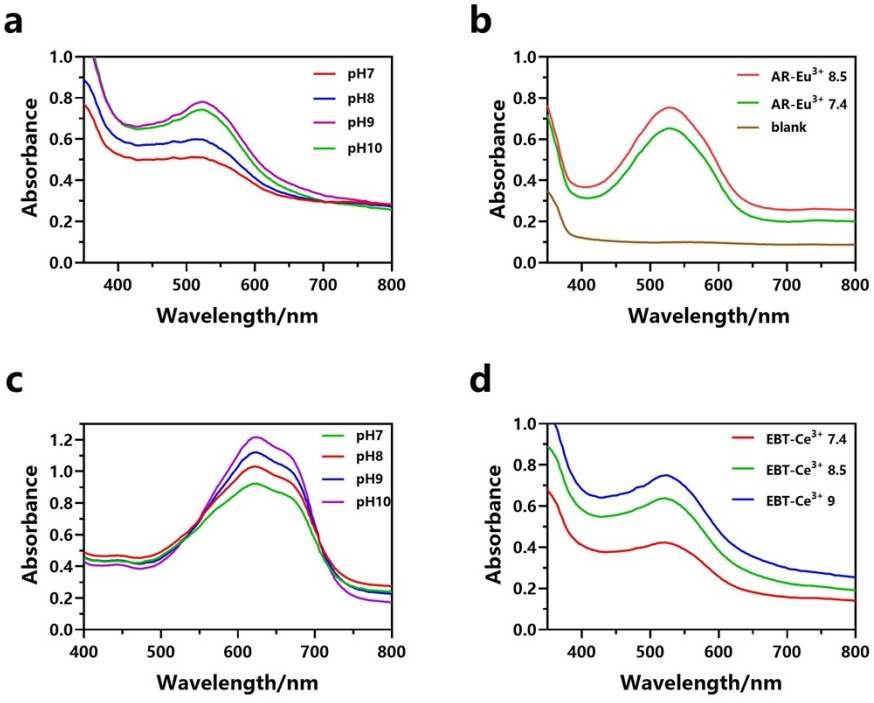

Figure S2. UV-Vis absorption curves of (a) AR at different pH; (b) AR-Eu^{3+} different pH; (c) EBT at different pH; (d) EBT-Ce^{3+} at different pH.

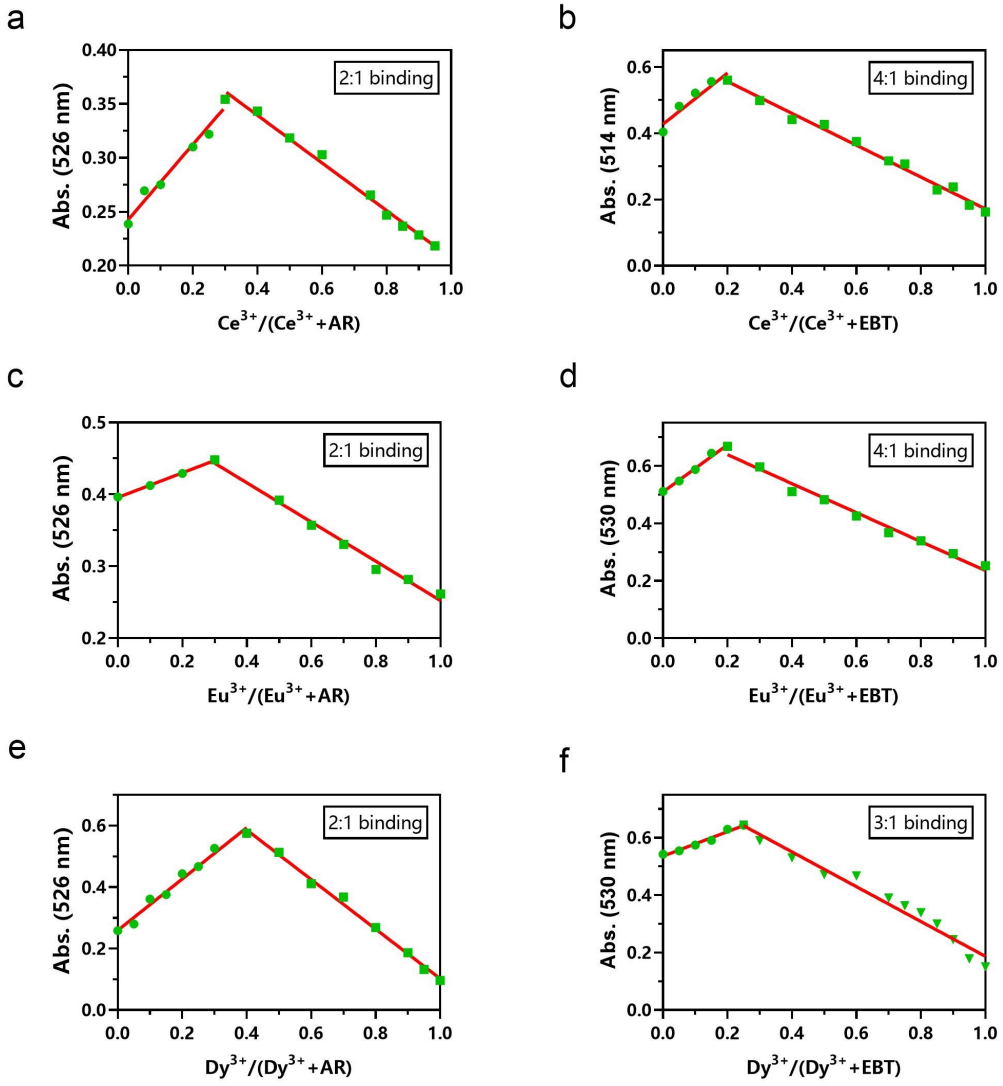

Figure S3. Job's plot for determination of stoichiometry of the complexation between AR/EBT and Ln^{3+} ions. (a) AR-Ce^{3+}; (b) EBT-Ce^{3+}; (c) AR-Eu^{3+}; (d) EBT-Eu^{3+}; (e) AR-Dy^{3+}; (f) EBT-Dy^{3+}.

Section 3: Pattern recognition analysis of lanthanide ions

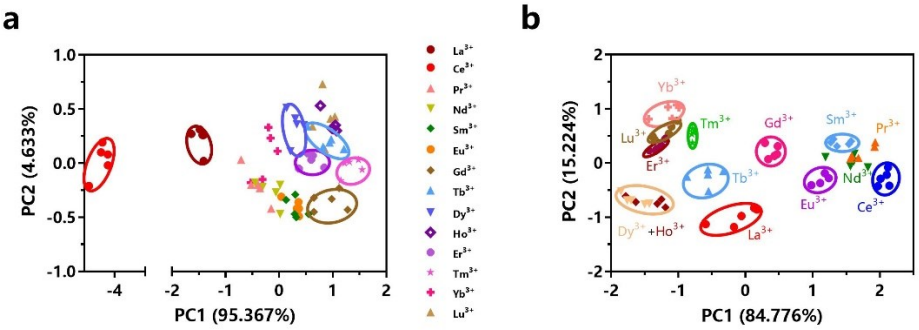

Figure S4. PCA plot for the discrimination of 14 lanthanide ions with (a) EBT at pH 7.4 and pH 8.5; (b) EBT at pH 7.4 and pH 8.5.

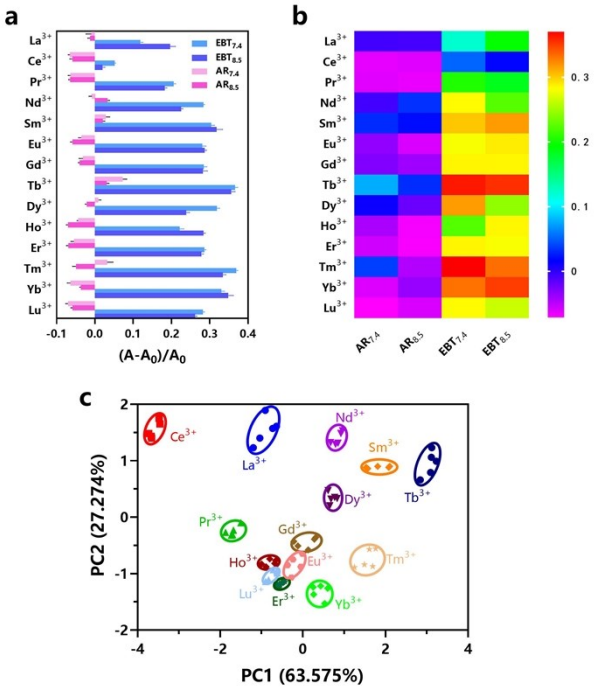

Figure S5. (a) The patterns of the 14 lanthanide ions based on the absorbance changes [(A-A_0)/A_0]; (b) Heat map based on the colorimetric patterns of complexometric indicators sensor array; (c) PCA plot for the discrimination of 14 lanthanide ions (10 μM).

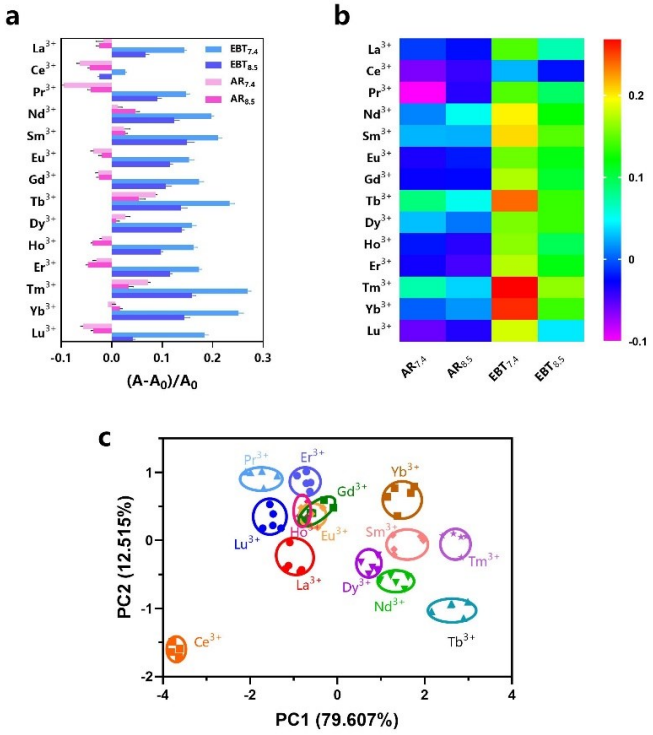

Figure S6. (a) The patterns of the 14 lanthanide ions based on the absorbance changes [$(A-A_0)/A_0$]; (b) Heat map based on the colorimetric patterns of complexometric indicators sensor array; (c) PCA plot for the discrimination of 14 lanthanide ions (5 μM).

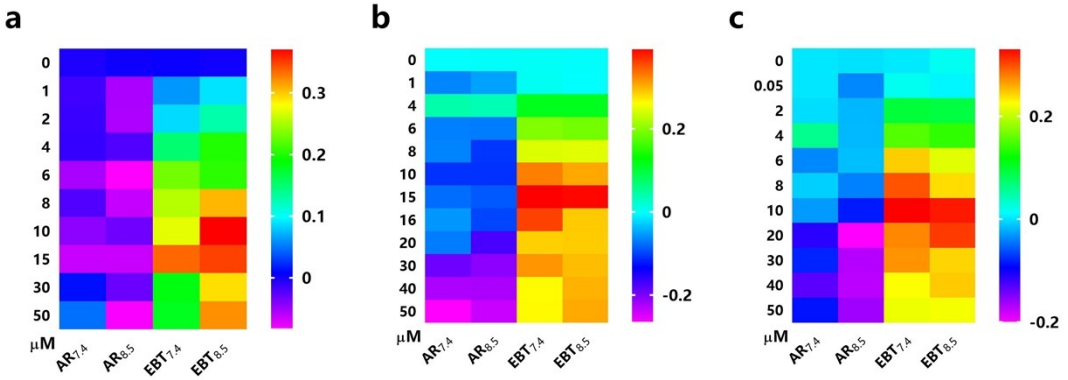

Figure S7. Heat map derived from the colorimetric patterns of AR/EBT sensors against (a) Ce^{3+}; (a) Dy^{3+}; (b)Tm^{3+}.

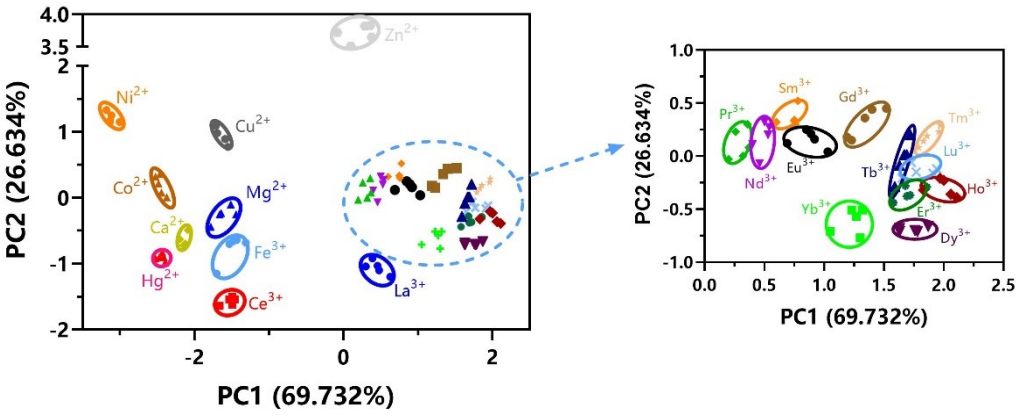

Figure S8. PCA score plots for AR/EBT sensors discerning lanthanide ions and metal ions (including Mg^{2+}, Ca^{2+}, Fe^{3+}, Co^{2+}, Ni^{2+}, Cu^{2+}, Zn^{2+}, Hg^{2+}).

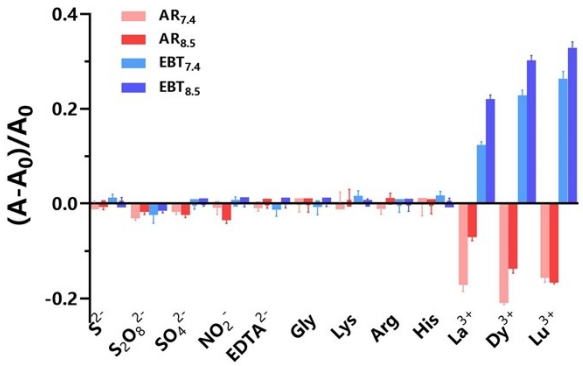

Figure S9. The patterns of anions, amino acids and lanthanide ions based on the absorbance changes [$(A-A_0)/A_0$].

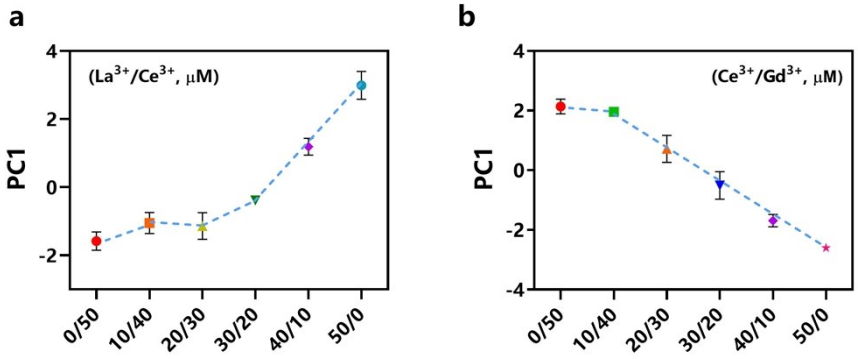

Figure S10. (a) Plot of PC1 vs the molar ratio of (a) La^{3+}/Ce^{3+}; (b)Ce^{3+}/Gd^{3+}.

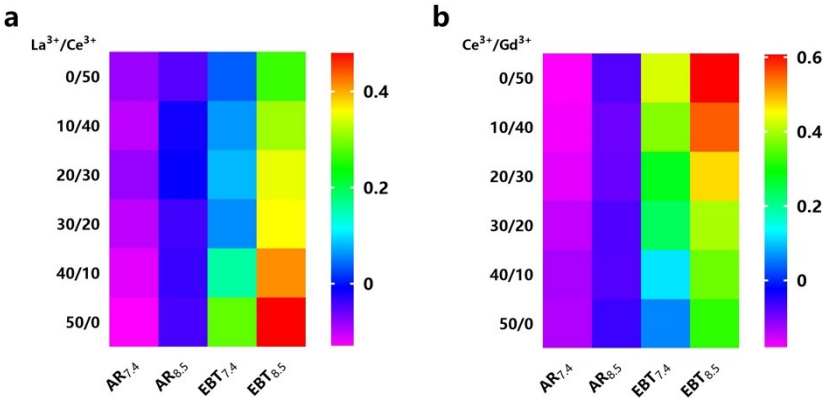

Figure S11. Heat map derived from the colorimetric response patterns of AR/EBT sensors toward different molar ratio of the mixture of (a) La^{3+}/Ce^{3+}; (b)Ce^{3+}/Gd^{3+}.

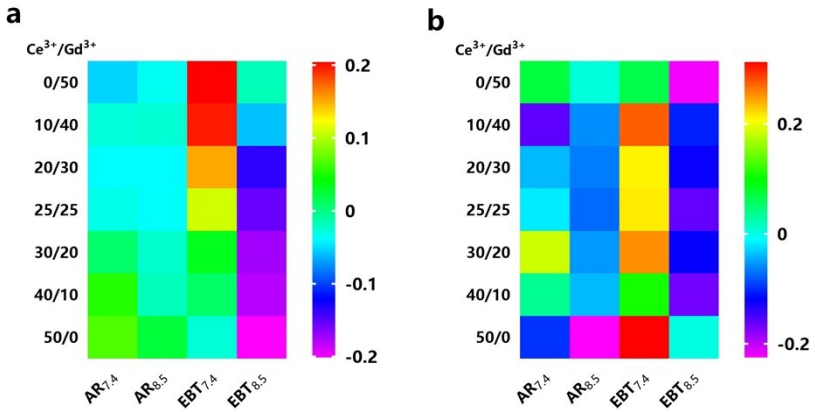

Figure S12. Heat map derived from the colorimetric response patterns of AR/EBT sensors against the mixture of Ce^{3+} and Gd^{3+} in (a) tap water; (b) river water.

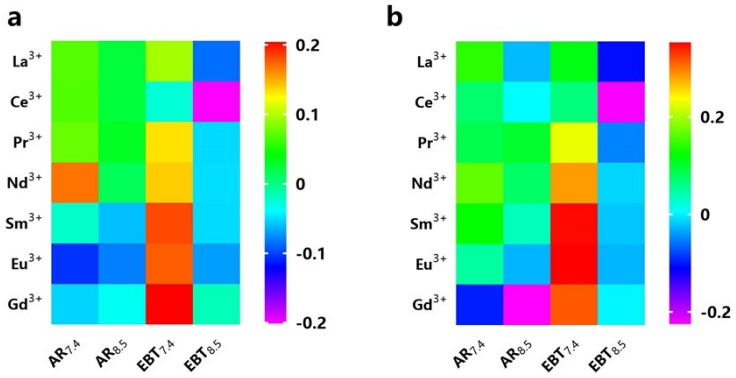

Figure S13. Heat map derived from the colorimetric response patterns of AR/EBT sensors against (a) tap water spiked with La^{3+}, Ce^{3+}, Pr^{3+}, Nd^{3+}, Sm^{3+}, Eu^{3+}, Gd^{3+}; (b) river water spiked with La^{3+}, Ce^{3+}, Pr^{3+}, Nd^{3+}, Sm^{3+}, Eu^{3+}, Gd^{3+}.

Table S1. Semi-quantitatively sensing lanthanide ions mixtures in real samples.

	Tap water				River water			
	Ce^{3+}/μM		Gd^{3+}/μM		Ce^{3+}/μM		Gd^{3+}/μM	
Entry	Actual	AR/EBT	Actual	AR/EBT	Actual	AR/EBT	Actual	AR/EBT
A	40	30-50	10	0-20	40	30-50	10	0-20
B	25	20-30	25	20-30	25	20-30	25	20-30
C	10	0-20	40	30-50	10	0-20	40	30-50